

# In Vitro Assessment of NSAIDs-Membrane Interactions: Significance for Pharmacological Actions

Cláudia Nunes • Daniela Lopes • Marina Pinheiro • Catarina Pereira-Leite • Salette Reis

Received: 12 February 2013 / Accepted: 19 April 2013 / Published online: 24 May 2013  
© Springer Science+Business Media New York 2013

## ABSTRACT

**Purpose** To study interactions between nonsteroidal anti-inflammatory drugs (NSAIDs) and membrane mimetic models.

**Methods** The interactions of indomethacin and nimesulide with liposomes of dipalmitoylphosphatidylcholine (DPPC) at two physiological pH conditions (pH 7.4 and 5.0) were investigated by time-resolved and steady-state fluorescence techniques and derivative ultraviolet/visible absorption spectrophotometry. Fluorescence quenching studies that assess the location of the drugs interacting with the membrane were carried out using labeled liposomes with trimethylammonium-diphenylhexatriene (TMA-DPH), a fluorescent probe with well-known membrane localization. Partition of the drugs within membranes was determined by calculating their partition coefficients ( $K_p$ ) between liposomes and water using derivative ultraviolet/visible absorption spectrophotometry in a temperature range of 37–50°C. The Van't Hoff analysis of the temperature dependence of  $K_p$  values allowed calculating the membrane-water variation of enthalpy ( $\Delta H_{w \rightarrow m}$ ) and entropy ( $\Delta S_{w \rightarrow m}$ ) and consequently the Gibbs free energy ( $\Delta G_{w \rightarrow m}$ ).

**Results** Results indicate that quenching, partitioning and thermodynamic parameters inherent to the interaction of the studied drugs with the membrane mimetic model are deeply dependent on the initial organization of the membrane, on the pH medium and on the physical properties of the drug.

**Conclusions** The interactions between NSAIDs and membranes are manifested as changes in the physical and thermodynamic properties of the bilayers. Depending on the composition and physical state of the membrane and the chemical structure of the NSAID, the interaction can support or prevent drug activity or toxicity.

**KEY WORDS** fluorescence • liposomes • NSAIDs • partition • thermodynamic parameters

## INTRODUCTION

The interaction with biomembranes represents a major contribution to the biological effect of drugs, once membranes are either the first barrier for cell internalization or the action site, where enzymes or receptors are the therapeutic targets. Although drugs bind to enzymes and receptors to exert their activity, increasing evidences highlight the prominent role of lipids in cell membranes and suggest that they might constitute novel targets for drugs whose pharmacological effects would be associated with the modulation of membrane biophysical properties (1,2). Various factors influence the behavior of drugs in cell membranes, such as partitioning, lipophilicity, pKa, among others (3). Nowadays, it is well-known that most of the perturbations that occur in complex biological membranes upon interaction with drug molecules can be studied using artificial membrane models such as liposomes (4), and can be quantified by valuable physicochemical techniques (4).

Drug-membrane interaction studies are particularly important in the case of nonsteroidal anti-inflammatory drugs (NSAIDs), since most NSAIDs are weakly acidic, amphiphilic compounds that interact strongly with lipid membranes (5–7). Hence, it is conceivable that the interaction of NSAIDs with lipid membranes is fundamental to elucidate their therapeutic and toxic effects. Indeed, NSAIDs control of pain and inflammation is due to the inhibition of a membrane associated enzyme, named cyclooxygenase (COX) (8,9). Furthermore, as location, structure and function of membrane-associated enzymes depend on cell membrane properties (10,11), such as fluidity (12), the mode of action of NSAIDs may be in great deal related to their

C. Nunes (✉) • D. Lopes • M. Pinheiro • C. Pereira-Leite • S. Reis  
REQUIMTE, Departamento de Ciências Químicas, Faculdade de Farmácia  
Universidade do Porto, Rua de Jorge Viterbo Ferreira, 228  
4050-313 Porto, Portugal  
e-mail: cdnunes@ff.up.pt

ability to interact with the lipid constituents of membranes and change their biophysical properties. Moreover, the surface of the mucosal barrier of gastrointestinal (GI) tract contains an extracellular lining of phosphatidylcholines (PCs) and related zwitterionic phospholipids (possibly a monolayer or multilayer) (13) that confers hydrophobic, non-wettable and acid resistant properties to this barrier, being however poorly resistant to the lipid-soluble NSAIDs (14,15). Therefore, the effects of NSAIDs on membranes, and specifically their ability to interact with surface-active phospholipids, as well as their effect on the lipid dynamic properties of membranes, may elucidate the effects of these drugs to compromise the integrity of gastric mucosal barrier (9,16,17). This knowledge gains deeper meaning considering the fact that NSAIDs are worldwide prescribed drugs for acute and chronic inflammatory conditions, and their continuous use has been associated with severe gastric toxicity.

According to the abovementioned, this work evaluates the interaction established between two effective NSAIDs, indomethacin and nimesulide, and large unilamellar vesicles (LUVs) made of dipalmitoylphosphatidylcholine (DPPC). In Table I is presented some structural information about the drugs used in this study.

LUVs of DPPC were the membrane model systems used in representation of: (i) a typical cell membrane (LUVs of DPPC in the fluid phase and at physiological pH of 7.4); and (ii) the protective membrane lining of the gastric mucosa (LUVs of DPPC in an ordered phase and at acidic pH of 5.0). These membrane model systems provide a simplified basis for the study of the NSAIDs-membrane interactions,

while maintaining all the fundamental properties of the biomembranes. Furthermore, DPPC was chosen as a suitable lipid to evaluate different aspects of NSAID-membrane interaction. DPPC is a common phospholipid used to determine the physicochemical and biological properties of cellular membranes (18). The gastric protective layer is composed of highly surface-active phospholipids, in particular phosphatidylcholines (19,20). Additionally, DPPC is an endogenous component of the joints and represents approximately 45% of the total synovial fluid lipid component being an appropriate lipid to mimic inflammatory articular conditions (21).

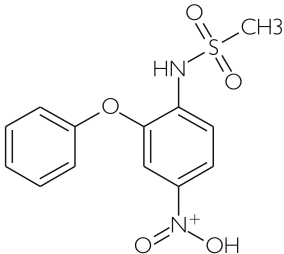
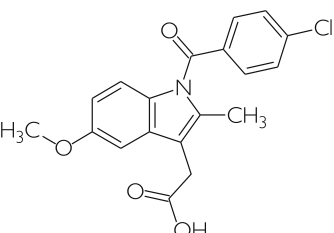
The study of NSAIDs-membrane interactions has been pursued by our research group (7,22–28). Although previous reported studies have already covered several aspects of NSAIDs-membrane interactions, the current work provides new and complementary information about these interactions. The studies performed include the determination of partition and location of NSAIDs in membrane using respectively, UV–vis derivative spectrophotometry and fluorescence techniques. The evaluation of the thermodynamic parameters inherent to the interaction established between drug and membrane was also carried out.

Partition of NSAIDs into lipid bilayers of biological membranes plays a significant role in their uptake, transport, bioavailability, and distribution (29). The primary mechanism of gastrointestinal absorption of the vast majority of drugs involves initial partitioning into cell membranes followed by passive diffusion (30). Hence, the thermodynamic parameters taken from partition may give important information about pharmacokinetic properties of NSAIDs.

Moreover, the interaction of NSAIDs was also evaluated in terms of their distribution across the lipid membrane by means of steady-state and time-resolved fluorescence measurements. The incorporation of the fluorescent probe trimethylammonium-diphenylhexatriene (TMA-DPH), which has a well-known positioning in the membrane (31), in the liposomes enabled the monitoring of fluorescence parameters such as intensity, lifetime and anisotropy upon interaction with the NSAIDs. Fluorescence quenching studies give information about the collision efficiency between probes and quenchers, which is then related with the location and diffusion properties of the quenchers, in this case indomethacin and nimesulide. On the other hand, fluorescence anisotropy data provide insights into the fluidity of the membrane, once they indicate the extent of the probe motions restriction by the anisotropic membrane environment.

In conclusion, besides unveiling the mechanisms of interaction of NSAIDs with membrane, this work may contribute to identify the biophysical aspects behind such interaction that might ultimately be helpful to the future development of more effective drugs with less undesirable side effects.

**Table I** Chemical Structures and pKa Values of the NSAIDs Investigated: Nimesulide and Indomethacin

	Molecular structure	pKa
Nimesulide		6.4
Indomethacin		4.5

## MATERIALS AND METHODS

### Materials

Indomethacin and nimesulide were obtained from Sigma Chemical Co. (St. Louis, MO, USA), and used without further purification. DPPC was purchased from Avanti Polar Lipids, Inc. (Alabama, USA) and TMA-DPH from Molecular Probes (Invitrogen Corporation, Carlsbad, California, USA). All other chemicals were purchased from Merck (Darmstadt, Germany).

Drug solutions were prepared either with Hepes buffer (10 mM, pH 7.4) or acetate buffer (0.2 M, pH 5.0). The ionic strength was adjusted to mimic physiological conditions with NaCl ( $I=0.1$  M). The buffers were prepared using double-deionized water (conductivity inferior to  $0.1 \mu\text{Scm}^{-1}$ ).

### Liposomes Preparation

Multilamellar vesicles (MLVs) were prepared by the classical method of the lipid film hydration (32). A DPPC solution, prepared with chloroform/methanol (3:2v/v), was evaporated to dryness with a nitrogen stream in a rotary evaporator. For TMA-DPH labeled liposomes used in the fluorescence measurements, the probe was co-dried with the lipid to give a lipid:probe molar ratio of 300:1. The resultant dried lipid film was dispersed in convenient buffer, either Hepes buffer or acetate buffer and the mixture was vortexed to yield MLVs. In order to obtain unilamellar liposomes (LUVs), the suspension was extruded 10 times through a polycarbonate filter with a pore diameter of 100 nm (33), at  $50^\circ\text{C}$  (temperature above the main phase transition temperature of the lipid).

### Determination of Partition Coefficients by Derivative UV/vis Absorption Spectrophotometry

Partition coefficients of NSAIDs were determined in LUVs of DPPC. Hepes or acetate buffered solutions of the two drugs were added to liposomes containing a fixed concentration of drug (40  $\mu\text{M}$  for indomethacin and nimesulide in Hepes buffer and 40  $\mu\text{M}$  for indomethacin and 25  $\mu\text{M}$  for nimesulide in acetate buffer) and increasing concentrations of DPPC (in the range of 50–1000  $\mu\text{M}$ ). The corresponding reference solutions were identically prepared in the absence of drug. The absorption spectra of samples and reference solutions were recorded at different temperatures above and beneath the lipid main phase transition temperature with a Perkin Elmer Lambda 45 UV/VIS spectrophotometer using quartz cells with 1 cm path length, in the 220–520 nm range. After measurements, each reference spectrum (background) was subtracted from the corresponding sample spectrum to obtain corrected absorption spectra. Derivative spectra were calculated using the Savitzky–Golay method (34) in which a second-order polynomial convolution of 13 points was employed (35).

### Drug Location Studies Evaluated by Fluorescence Quenching

Quenching studies included fluorescence steady-state and fluorescence time-resolved measurements. These studies were carried out by incubation of drugs with TMA-DPH labeled liposomes. Samples contained a fixed concentration of DPPC (500  $\mu\text{M}$ ) and increasing concentrations of NSAIDs (0 – 100  $\mu\text{M}$ ). Before fluorescence measurements, the resulting suspensions were incubated in the dark for 30 min at a temperature above the lipid main phase transition so that NSAIDs could reach the partition equilibrium between the lipid membranes and the aqueous medium. Fluorescence measurements were carried out at four controlled temperatures for each pH value from  $37^\circ\text{C}$  to  $47^\circ\text{C}$ , at excitation and emission wavelengths defined as 361 nm and 427 nm, respectively.

Fluorescence steady-state measurements were performed in a Perkin Elmer LS-50B spectrofluorimeter equipped with a constant temperature cell holder. All data were recorded in a 1 cm path length cuvette. For each measurement, fluorescence emission was automatically acquired during 30 s. Fluorescence intensity values were corrected for inner filter effects at the excitation wavelength (36).

Fluorescence time-resolved measurements were made with a Fluorolog Tau-3 Lifetime system. Modulation frequencies were acquired between 6 and 200 MHz. Integration time was 10 s. Manual slits were 0.5 mm, slits for excitation monochromator were 7.0 mm (side entrance) and 0.7 mm (side exit) and for emission monochromator 7.0 mm (side entrance) and 7.0 mm (side exit). The fluorescence emission was detected with a  $90^\circ$  scattering geometry. All measurements were made using Ludox as a reference standard ( $\tau=0.00$  ns).

### Membrane Fluidity Studies Evaluated by Fluorescence Anisotropy

Steady-state fluorescence anisotropy measurements ( $r_{ss}$ ) were performed in the same Perkin Elmer LS-50B spectrofluorimeter with polarizers inserted (excitation/emission wavelengths were set as described). The sample was excited with vertically polarized light and fluorescence intensities were recorded with the analyzing polarizer oriented parallel ( $I_{||}$ ) and perpendicular ( $I_{\perp}$ ) to the excitation polarizer. Data were collected after an integration time of 30 s.

## RESULTS AND DISCUSSION

### Determination of Partition Coefficients by Derivative UV/vis Absorption Spectrophotometry

The partition coefficient ( $K_p$ ) of the NSAIDs was studied in liposome-water system once, octanol-water system does not

mimic the interfacial character of the membrane phospholipid bilayer and the influence of the ionic interaction of charged drug molecules with the polar phospholipid headgroups [3].  $K_p$  was assessed by UV–Vis derivative spectrophotometry without physical phase separation. The analysis is based on the change of spectral characteristics of the drug when it permeates from the aqueous to the lipid phase. Figure 1a illustrates the spectral shifts of the  $\lambda_{\max}$  with increasing lipid concentration, an observation that provides a clear indication that the drug (in this case, indomethacin) partitions from the aqueous to the lipid media.

It is also possible to observe in Fig. 1a that the references' spectra (black lines) give intense absorption signals arising from light scattered by the lipid vesicles, which difficult the obtainment of a correct baseline even after subtracting the background from the absorbance spectra.

Nevertheless, using second-derivative spectrophotometry (Fig. 1b), the effect of background signals is eliminated and the resolution of the absorption signals is improved by sharpening the bands. Furthermore, the derivative spectra also exhibit the  $\lambda_{\max}$  shift and additionally show distinct isosbestic points, confirming the complete elimination of the residual background signal effects of the lipid vesicles (35,37). The existence of the derivative isosbestic points also indicates that indomethacin is located in the two environments: in the aqueous media and in the liposome media. Similar results were obtained for all the experiments.

$K_p$  was obtained from the experimental values of lipid concentration ( $[L]$ ) and the second derivative intensity of the absorbance values (at wavelengths where the scattering is eliminated) by applying a non-linear least-squares regression method, described by Eq. (1):

$$D_T = D_w + \frac{(D_m - D_w)K_p[L]V_0}{1 + K_p[L]V_0} \quad (1)$$

where  $D_T$ ,  $D_w$ , and  $D_m$  are respectively the total, aqueous and membrane second derivative intensities obtained from

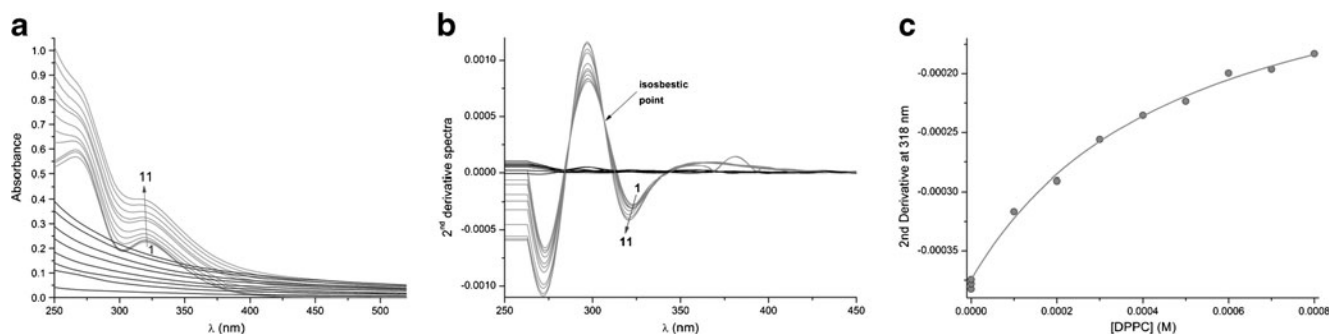
the absorbance of the drug;  $K_p$  is the partition coefficient; and  $V_0$  is the lipid molar volume of DPPC ( $0.70 \text{ Lmol}^{-1}$ ) (38).

Figure 1c shows, as an example, the best fit of the Eq. (1) to the second-derivative spectrophotometric data, collected at  $\lambda = 318 \text{ nm}$ , of indomethacin and with different concentrations of DPPC liposomes.

The values of  $K_p$  and their experimental error obtained for both drugs, at pH 5.0 and pH 7.4 and for several temperatures are listed in Table II.

The gathered  $K_p$  values obtained with both drugs indicate that the membrane partition of indomethacin is higher than nimesulide, at both pHs. This result suggests that the distribution of the drugs between the membrane and aqueous phase is different from drug to drug even for those sharing the similar pharmacological activity. Drug distribution depends on several properties of the drug, such as their structure, degree of ionization and also on some properties of the membrane like the molecular packing of the lipids.

At pH 5.0, both drugs present higher  $K_p$  values than at pH 7.4. This might be attributed to the fact that at lower pH the drugs are less ionized and it is expected that the neutral forms of the drugs are able to permeate more efficiently into the lipid membrane. This increased partition of neutral forms of NSAIDs has already been demonstrated for some oxicams (39). For the charged forms of the drugs at pH 7.4, the membrane partition is most probably assured by drug-membrane interactions of electrostatic nature, between the negatively charged drugs and the positively charged choline moiety of DPPC. Although choline group is a quaternary amine, not easily accessible due to their methyl groups, several other studies have already demonstrated that due to a molecule rearrangement the negatively charged NSAIDs interact with the positively charged choline (13,25,27,40). Particularly in a work by Lichtenberger (13), the molecular dynamics simulations showed that anionic NSAIDs ( $\text{pH} > \text{pKa}$ ) partition is most favourably into the



**Fig. 1** Absorption spectra (**a**) and second-derivative spectra (**b**) of indomethacin at pH 5.0 ( $40 \mu\text{M}$ ) incubated in LUVs of DPPC in acetate buffer at  $45^\circ\text{C}$  (gray lines) and LUVs of DPPC without drug (black lines) at increasing lipid concentrations from one to eleven, which represents the increasing concentrations of DPPC. The graphic (**c**) represents the fitting curve to experimental second-derivative spectrophotometric data ( $D_t$  vs.  $[\text{DPPC}]$ ) using a nonlinear least squares regression method at wavelength  $318 \text{ nm}$  where the scattering is eliminated.

**Table II** Partition Coefficients of Indomethacin and Nimesulide Obtained in a Biphasic Membrane/Aqueous System (LUVs of DPPC and Buffers of pH 7.4 and 5.0), at Several Temperatures by Derivative Spectrophotometry. Values Represent the Mean and Standard Deviation of at Least Three Independent Assays

pH	Temperature (°C)	$K_p$ ( $M^{-1}$ )	
		Indomethacin	Nimesulide
5.0	37.0 ± 0.1	1717 ± 38	195 ± 22
	43.0 ± 0.1	2182 ± 4	655 ± 123
	45.0 ± 0.1	3360 ± 168	1021 ± 147
	48.0 ± 0.1	6323 ± 105	1772 ± 162
	50.0 ± 0.1	9574 ± 1010	2826 ± 193
7.4	37.0 ± 0.1	254 ± 13	98 ± 10
	43.0 ± 0.1	327 ± 12	279 ± 28
	45.0 ± 0.1	649 ± 14	487 ± 74
	48.0 ± 0.1	1387 ± 98	1128 ± 110
	50.0 ± 0.1	1909 ± 178	1288 ± 128

headgroup region of the phospholipid bilayer, due to electrostatic interactions with the positively-charged quaternary ammonium component of choline.

Also for both drugs and pHs, the partition at the fluid phase is greater than at the gel phase, once the lipids are much more organized and packed at this latter phase making more difficult the penetration of drugs within the membrane.

### Calculations of Thermodynamic Parameters

The Van't Hoff analysis of the temperature dependence of  $K_p$  values allowed calculating the membrane-water variation of enthalpy ( $\Delta H_{w \rightarrow m}$ ) and entropy ( $\Delta S_{w \rightarrow m}$ ) and consequently the Gibbs free energy ( $\Delta G_{w \rightarrow m}$ ). The temperature dependence was used to obtain the variation of enthalpy and entropy involved in drug's partition, which were determined from the slope and interception of the Van't Hoff linear plot described by the following equation:

$$\ln(K_p) = -\frac{\Delta H}{RT} + \frac{\Delta S}{R} \quad (2)$$

where  $R$  is the gas constant ( $8.314 \text{ J mol}^{-1} \text{ K}^{-1}$ ) and  $T$  is the temperature in Kelvin.

The free energy of partition was calculated from the enthalpy and entropy values obtained by the previous expression by the well-known relation:

$$\Delta G = \Delta H - T\Delta S \quad (3)$$

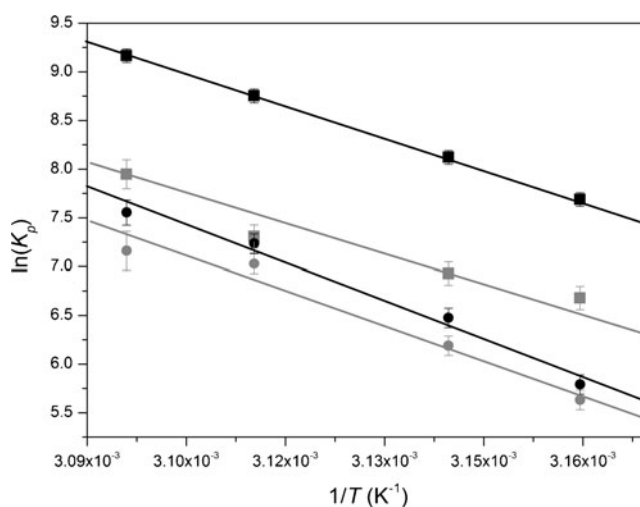
The thermodynamic parameters obtained for nimesulide and indomethacin partition between aqueous phase and the DPPC bilayer in both pH values and at the  $L_\alpha$  phase were calculated based on the temperature dependence of  $K_p$

value, and the gathered results are shown in Fig. 2 and Table III.

The enthalpic and entropic changes regarding the partition of the drugs between aqueous phase and the lipid bilayer are intimately related with the energetic requirements and the molecular randomness. Since the packing and the molecular arrangement is deeply modified when the lipid goes from the gel phase to the fluid phase; the partition behavior as well as its thermodynamic aspects should be independently considered in each phase (41).

The negative values obtained for free energy ( $\Delta G_{w \rightarrow m}$ ) presented in Table III mean that the interaction process of nimesulide and indomethacin with DPPC bilayers is spontaneous. For all the cases, it can be seen that as temperature rises, the  $\Delta G_{w \rightarrow m}$  becomes more negative, which was expected once the lipid bilayer is more fluid and disorganized and thereby more prone to drug interaction. A more negative value of free energy is also verified for both drugs at pH 7.4 than at pH 5.0, contrasting to the lower partition of drugs at pH 7.4, which can be related to the nature of the interaction involved. While at pH 7.4 the drugs are negatively charged and thus, they may electrostatically interact with the polar headgroups of phospholipids, at pH 5.0 the neutral forms of the drugs may further diffuse into the bilayer and this penetration process may require a higher amount of energy.

All of the Van't Hoff plots were linear and presented a high coefficient of determination (superior than 0.96). The negative slopes, *i.e.*, positive variation of enthalpy values from water to membrane ( $\Delta H_{w \rightarrow m}$ ), show that the partition of the NSAIDs studied is an endothermic process. Indeed, it is necessary to supply energy to separate the lipid molecules, thereby creating space in the membrane medium to

**Fig. 2** Van't Hoff Plots of indomethacin and nimesulide in LUVs of DPPC at pH 7.4 and 5.0. The black symbols and lines represent indomethacin and the grey ones nimesulide. The squares are the results at pH 5.0 and the circles at pH 7.4.



**Table III** Thermodynamic Parameters of the Partition of Indomethacin and Nimesulide in a Biphasic Membrane/Aqueous System (LUVs of DPPC and Buffers of pH 7.4 and 5.0), at the  $L_\alpha$  Phase

	Temperature (K)	$\Delta G_{w \rightarrow m}$ (KJ.mol <sup>-1</sup> )	$\Delta H_{w \rightarrow m}$ (KJ.mol <sup>-1</sup> )	$\Delta S_{w \rightarrow m}$ (J.mol <sup>-1</sup> .K <sup>-1</sup> )
Indomethacin pH 5.0	316	-5.48	2.59	9.13
	318	-5.49		
	321	-5.52		
	323	-5.54		
Indomethacin pH 7.4	316	-6.42	3.10	10.5
	318	-6.44		
	321	-6.47		
	323	-6.49		
Nimesulide pH 5.0	316	-5.16	2.46	8.54
	318	-5.18		
	321	-5.20		
	323	-5.22		
Nimesulide pH 7.4	316	-5.81	2.80	9.54
	318	-5.83		
	321	-5.86		
	323	-5.88		

accommodate the drugs, allowing their transference from the aqueous to the lipid phase. When the drug molecules are accommodated in the lipid phase an amount of energy is released due to drug-membrane interactions. This event implies an entropy increase in the lipid medium due to the mixing process. Hence, if the drug molecules have higher interaction with the membrane it is expected to have higher values of  $\Delta H_{w \rightarrow m}$  and  $\Delta S_{w \rightarrow m}$ . This is in fact what happens: the  $\Delta S_{w \rightarrow m}$  and  $\Delta H_{w \rightarrow m}$  values are higher for both drugs at physiological pH, despite the values of  $K_p$  being smaller at this pH. Again the justification lies on the fact that at pH 7.4 the drugs are charged and the drug-membrane interaction is expected to be of electrostatic nature, involving the negatively charged groups of the NSAIDs and the positively charged choline of DPPC, which justifies the higher entropy and energy consuming with a lower  $K_p$ .

### Drug-Bilayer Interaction Studies by Fluorescence Quenching

The extent of fluorescence quenching of a membrane bound fluorophore provides a measure of the accessibility of the quencher to the fluorophore. Hence, if the molecular location of a fluorophore within membranes is known with certainty, quenching studies can be used to assess the location of quenchers in membranes and the permeability of membrane to quenchers (42). In this case, the quenching efficiency of indomethacin and nimesulide was evaluated by the addition of increasing amounts of drug to liposome suspensions with incorporated TMA-DPH probe. The

location and orientation of this probe within the lipid bilayer is reported as being anchored in the phospholipids polar heads and aligned parallel to the acyl chains (43).

The efficiency to quench the fluorophore depends on the proximity of the quencher. Once the fluorophore is inserted at the membrane level, only the drug that partitions into the lipid phase will be able to act as a quencher. Therefore, to proceed with the determination of quenching efficiency, it is first needed to determine the effective quencher concentration, *i.e.* the concentration of quencher that is able to partition into the membrane ( $[Q]_m$ ), which is calculated from the total drug concentration ( $[Q]_T$ ) and from the drug's partition coefficient ( $K_p$ ), as described by the following equation:

$$[Q]_m = \frac{K_p[Q]_T}{K_p\alpha_m + (1 - \alpha_m)} \quad (4)$$

where  $\alpha_m$  is the volume fraction of membrane phase ( $\alpha_m = V_m/V_T$ ;  $V_m$  and  $V_T$  represent the volumes of the membrane and water phases, respectively).

Both drugs at the two pH conditions and for all the studied temperatures have effectively quenched the TMA-DPH probe. Moreover, the wavelength corresponding to the absorption band of the probe does not change in the presence of quencher and also, no additional band was observed at a longer wavelength, which points to a quenching that is dynamic or collisional in nature. Collisional quenching of fluorescence is described by the Stern-Volmer equation (42):

$$\frac{I_0}{I} = 1 + K_{SV}[Q]_m = \frac{\tau_0}{\tau} \quad (5)$$

In this equation  $I_0$  and  $I$  are the fluorescence intensities in the absence and presence of quencher, respectively;  $K_{SV}$  is the quenching constant, called the Stern-Volmer constant;  $\tau_0$  and  $\tau$  are the lifetime of the fluorophore in the absence and presence of quencher, respectively. This equation illustrates an important characteristic of collisional quenching, which is an equivalent decrease in fluorescence intensity and lifetime.

If the quenching is purely collisional,  $I_0/I - 1$  is expected to vary linearly with the concentration of quencher. It is important to note that the observation of a linear Stern-Volmer plot does not prove that collisional quenching of fluorescence has occurred. Therefore, to evaluate the mechanism of quenching and distinguish between a collisional and a static quenching, studies at different temperatures were performed for each pH. If the quenching is purely collisional, higher temperatures will result in faster diffusion and hence, in larger amounts of collisional quenching, leading to higher  $K_{SV}$  values. On the other hand, in the case of static quenching, higher temperatures will result in the dissociation of weakly bound complexes, and thus, will lead to lower values of  $K_{SV}$ , as shown in Fig. 3.

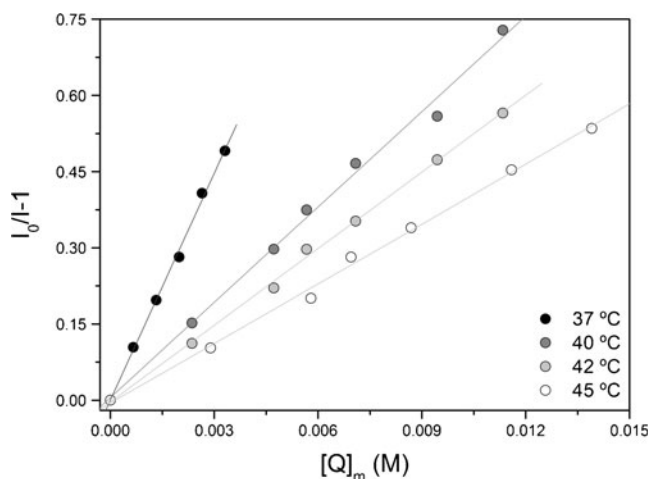


**Fig. 3** Stern–Volmer plots of fluorescence quenching of the probe TMA-DPH in LUVs of DPPC at pH 5.0 by increasing concentrations (M) of the quencher nimesulide at 37 °C (●), 40 °C (◐), 42 °C (◑) and 45 °C (○).

Nevertheless, the measurement of fluorescence lifetimes is the most accurate method to distinguish static and dynamic quenching. Complexed fluorophores are nonfluorescent, and the observed fluorescence is just from the uncomplexed fluorophores. The uncomplexed fraction is unperturbed, and hence the lifetime is  $\tau_0$ . Therefore, for static quenching  $\tau_0/\tau=1$ . In contrast, for dynamic quenching  $I_0/I=\tau_0/\tau$  (42).

In many cases the fluorescent probe can be quenched both by collisions and by complex formation with the same quencher. The characteristic feature of the Stern-Volmer plots in such circumstances is an upward curvature. The dynamic portion of the observed quenching is determined by lifetime measurements, through the following equation:

$$\frac{\tau_0}{\tau} = 1 + K_D[Q] \quad (6)$$

Afterwards, knowing the dynamic component, the static contribution may be found by linearization of the following equation (42):

$$\frac{I_0}{I} \times \frac{1}{1 + K_D[Q]_m} = 1 + K_S[Q]_m \quad (7)$$

This modified form of the Stern-Volmer equation is second order in  $[Q]_m$ , which accounts for the upward curvature observed when both static and dynamic quenching occur for the same fluorophore. In Fig. 4 is displayed a typical example for this kind of behavior.

The positive deviation of the Stern-Volmer plots can also be interpreted in terms of a ‘sphere of action’ quenching model. According to this model, an instantaneous quenching occurs if the quencher molecule is adjacent to the fluorophore at the moment of excitation. When the fluorophore and quencher are that close, there is a high

probability of the quenching occurs before both molecules diffuse apart. As the quencher concentration increases, the probability of a quencher to be within the sphere of action of the fluorophore at the moment of excitation also increases. Hence, only a certain fraction of the excited fluorophore is quenched by Stern–Volmer collisional mechanism. Moreover, this model assumes that, if the quencher is located inside a spherical volume ( $V$ ) adjacent to the fluorophore, the probability for the quencher to be inside this volume at the time of excitation depends on the volume itself and on the quencher concentration ( $[Q]_m$ ), as it is described by the modified Stern-Volmer equation (42):

$$\ln\left(\frac{I_0\tau}{I\tau_0}\right) = V[Q]_m \quad (8)$$

In Fig. 5 is presented one example of the sphere of action model, where it is possible to see the application of the previous equation that leads to the determination of the volume of the sphere (Fig. 5a). The volume of the sphere is then applied in Eq. (9) in order to get the  $K_{SV}$  value (Fig. 5b):

$$\frac{I_0}{Ie^{V[Q]}} = 1 + K_{SV}[Q] = \frac{\tau_0}{\tau} \quad (9)$$

Moreover, the efficiency of the quenching or the accessibility of the fluorophores can also be assessed by the calculation of the bimolecular quenching rate constant (42):

$$K_q = \frac{K_D}{\tau_0} \quad (10)$$

If the quenching is known to be dynamic, the Stern-Volmer constant will be represented by  $K_D$ , otherwise this constant will be described as  $K_{SV}$ . Diffusion-controlled quenching typically results in values of near  $1 \times 10^{10} \text{ M}^{-1}\text{s}^{-1}$ . Values of  $K_q$  smaller than the diffusion-controlled value can result from steric shielding of the fluorophore or a low quenching efficiency. Apparent values of  $K_q$  larger than the diffusion-controlled limit usually indicate some type of binding interaction (42).

According to the aforementioned analysis of the quenching behavior of the drugs studied, the quenching parameters are presented in Table IV.

From the analysis of Table IV, it is possible to conclude that the quenching process is deeply dependent on the pH (which affects the degree of ionization of the drug), on the structure of the quencher and even on the initial state of the lipid membrane (either in the  $L_\beta'$  or the  $L_\alpha$  phase). The  $K_{SV}$  values show that, in the case of indomethacin at pH 5.0 and 7.4 and nimesulide at pH 5.0, the quenching process results from dynamic and static interactions, but with a dominant static component, once the values decrease with the increase of temperature, which is indicative of complex dissociation.

Concerning nimesulide at pH 5.0, the ‘sphere of action’ model is well suited to define the quenching process, once

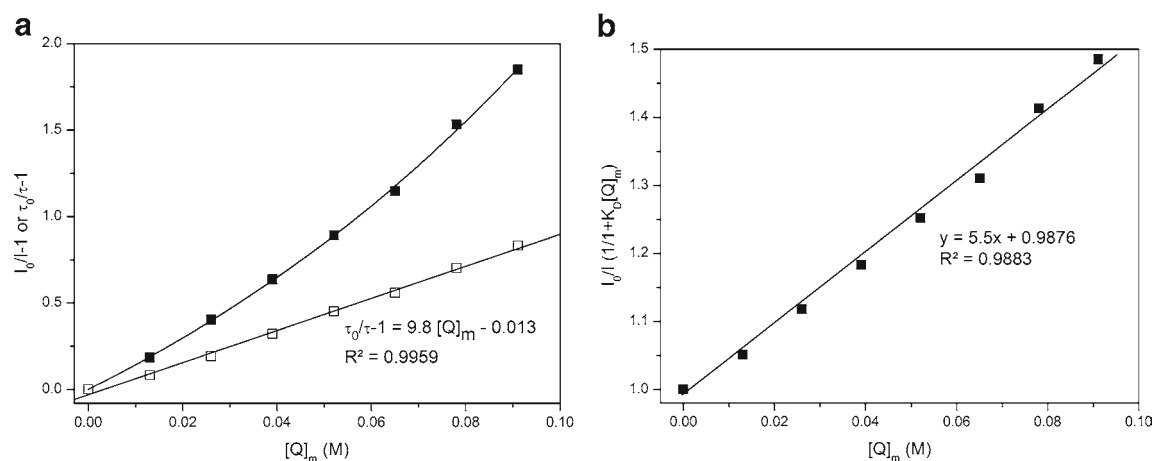


**Fig. 4** Stern–Volmer plots of the probe TMA-DPH in LUVs of DPPC at pH 5.0 at 45°C by increasing concentrations (M) of indomethacin. In **(a)** solid symbols represent Stern–Volmer plot obtained by steady-state fluorescence measurements ( $I_0/I - 1$ ) and open symbols represent Stern–Volmer plot obtained by lifetime fluorescence measurements ( $\tau_0/\tau - 1$ ). **(b)** Linearization for simultaneous dynamic and collisional quenching, taking the  $K_D$  value from the linearization of the lifetimes presented in **(a)**.

that a good correlation is obtained between the value of  $K_{SV}$  obtained from the sphere of action model (Eq. 9) and the  $K_D$  value calculated from the experimental lifetime Stern–Volmer plots, as it can be seen in Fig. 5b.

For both drugs and at the two pHs, the efficiency of quenching is higher for lower temperatures, as indicated by the higher  $K_{SV}$  values obtained. The quenching process in all cases has a predominant static component or a ‘sphere of action’ performance (with the same behavior as static) and a tight packing favors the formation of a complex.

### Membrane Fluidity Studies by Fluorescence Anisotropy Measurements

Steady-state fluorescence anisotropy measurements have been widely used to study the effect of several compounds in cellular

membrane fluidity (44–47). The results are often analyzed according to the Perrin equation. However, Perrin equation must be only applied to isotropic rotation of a fluorophore and it is not applicable to the hindered rotation of the probes in anisotropic lipid bilayers. Moreover, the data can be influenced by the probe itself. Indeed, it is possible that the observed changes in anisotropy may be caused not only by changes in membrane microviscosity, but also by changes in the excited-state lifetime of the fluorophore, which can be eliminated using corrected anisotropy values ( $r'$ ) given by (6):

$$r' = \frac{\theta + \tau_0}{\theta + \tau} \times r_{ss} \quad (11)$$

where  $\theta$  is the rotational relaxation time of the probe,  $r_{ss}$  the experimental anisotropy values and  $\tau_0$  and  $\tau$  are the experimental values of the lifetime in the absence and

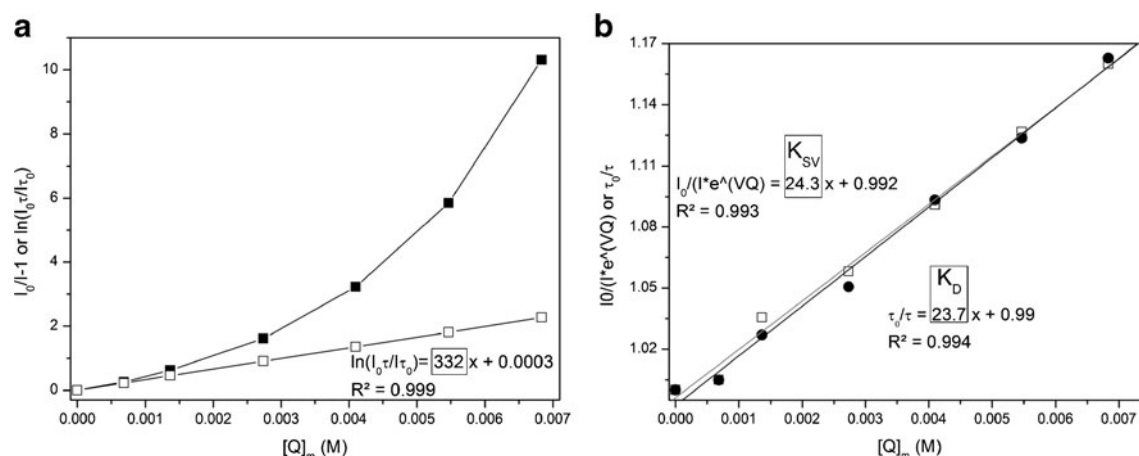


**Fig. 5** **(a)** Fluorescence quenching of TMA-DPH probe in LUVs of DPPC by increasing concentrations of nimesulide at pH 7.4 and 37°C and respective application of the mathematical model “sphere of action”. **(b)** Linearization of the  $K_D$  and  $K_{SV}$



**Table IV** Fluorescence Quenching Parameters Calculated from the Quenching of TMA-DPH by Indomethacin and Nimesulide in LUVs of DPPC at Different Temperatures and Two pH Values. Fluorescence Quenching Parameters Include Values of the Dynamic Constant ( $K_D$ ), the Static Constant ( $K_S$ ), the Stern–Volmer constant ( $K_{SV}$ ), the Bimolecular Quenching Constant ( $K_q$ ) and the Sphere of Action Volume ( $V$ ) and Radius ( $r$ ) Obtained from Measurements

	T (°C)	pH	$K_D$ (M <sup>-1</sup> )	$K_q \times 10^{-8}$ (M <sup>-1</sup> s <sup>-1</sup> )	$K_S$ (M <sup>-1</sup> )	$K_{SV}$ (M <sup>-1</sup> )	V esf. (exp.)	r (nm)
Indomethacin	37	5.0	13.7 ± 0.4	2.1 ± 0.6	13.9 ± 0.2	27.6 ± 0.6	–	–
	40		11.6 ± 0.5	2.1 ± 0.8	7.04 ± 0.09	18.6 ± 0.6	–	–
	42		9.5 ± 0.6	2.3 ± 0.7	8.0 ± 0.3	17.5 ± 0.9	–	–
	45		9.8 ± 0.4	2.6 ± 0.5	5.5 ± 0.2	15.3 ± 0.6	–	–
Indomethacin	37	7.4	11.7 ± 0.3	1.6 ± 0.5	48.1 ± 0.7	59.8 ± 0.8	–	–
	42		13.2 ± 0.4	2.9 ± 0.7	27.2 ± 0.7	40 ± 1	–	–
	45		7.1 ± 0.3	1.8 ± 0.7	7.4 ± 0.3	14.5 ± 0.6	–	–
	47		3.9 ± 0.1	1.1 ± 0.3	1.81 ± 0.06	5.7 ± 0.2	–	–
Nimesulide	37	5.0	–	–	148 ± 4	148 ± 4	–	–
	40		–	–	62 ± 2	62 ± 2	–	–
	42		–	–	50.3 ± 0.9	50.3 ± 0.9	–	–
	45		17 ± 2	4 ± 2	17 ± 1	34 ± 3	–	–
Nimesulide	37	7.4	24.3 ± 0.9	3 ± 1	–	23.7 ± 0.8	332 ± 1	5 ± 1
	42		24 ± 2	5 ± 2	–	24 ± 2	177.2 ± 0.9	4.1 ± 0.9
	45		9.3 ± 0.5	2.3 ± 0.9	–	9.2 ± 0.3	79.0 ± 0.5	3.1 ± 0.5
	47		4.3 ± 0.2	1.3 ± 0.4	–	4.3 ± 0.3	33.8 ± 0.1	2.4 ± 0.1

presence of the quencher, respectively. The difference between  $r_{ss}$  and  $r'$  provides the real variation of anisotropy caused by the drug, without the effect of its intrinsic variation due to the decrease of probe fluorescence lifetime. Furthermore, it is possible to convert this difference in the fluidizing effect, taking into account the real variation of anisotropy in the absence of the quencher ( $r'_0$ ):

$$\text{fluidizing effect}(\%) = \frac{r_{ss} - r'}{r'_0} \times 100 \quad (12)$$

In agreement with a previously reported study with another superficial probe, the effect of nimesulide as a

membrane fluidizer is considered negligible because no evident perturbation on the motion of the probe was observed (45). In contrast, indomethacin at pH 5.0 has led to a maximum fluidizing effect of about 70% (Fig. 6), while at pH 7.4, the fluidizing effect was of about 20% (data not shown).

## CONCLUSIONS

The overall results of this work establish at a molecular level, that NSAIDs markedly interact with phospholipid

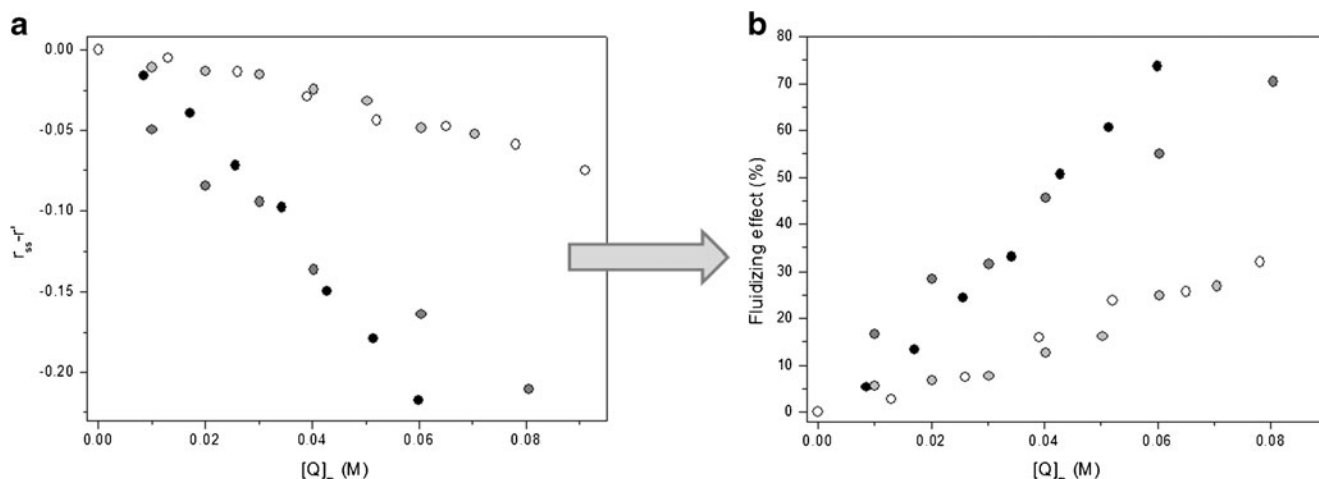


**Fig. 6** Effect of increasing membrane concentrations of indomethacin at pH 5.0 at 37°C (●), 40°C (◐), 42°C (○) and 45°C (○) on (a) the effective anisotropy variation ( $r_{ss} - r'$ ) of the TMA-DPH probe incorporated in LUVs of DPPC and (b) respective fluidizing effect.

membranes and change their properties. These findings can be directly correlated with NSAIDs therapeutic and toxic effects.

Our results show that at the fluid phase the partition of both indomethacin and nimesulide is higher at pH 5.0 than at pH 7.4. Once pH 5.0 is the characteristic pH of inflamed tissues where NSAIDs exert their therapeutic action, the higher partition of both drugs at this pH is coherent with their efficiency as anti-inflammatory drugs, enabling them to interact with the membrane-associated enzyme COX.

The gel phase of the membranes has also significance, once ordered domains are also important for membrane function and lipid gel phase simulates the gastric protective gel layer. At lower temperatures (more ordered membrane) the partition of both drugs pH 5.0 is much higher than that at pH 7.4. The fluorescence quenching studies revealed that for both pH values, the drugs were more effective quenchers at lower temperatures, which confirms the presence of NSAIDs even at a more ordered lipid bilayer. These observations together with the fluidity studies suggest that at acidic pH, also characteristic of the gastric mucosa, there is a significant interaction of NSAIDs with the membrane, which constitutes a biophysical support for the reported detrimental effects of NSAIDs on the gastric mucosa. It should be also mentioned, that despite both drugs are able to interact with membranes at both pH values and at both lipid phases, nimesulide effect as a membrane fluidizer was considered negligible. In contrast, indomethacin at pH 5.0 has led to a maximum fluidizing effect of about 70% and 20% at pH 7.4. These results provide additional biophysical arguments to support the higher GI toxicity presented by indomethacin, while nimesulide is considered a safer NSAID. Indeed, the fluidizing effect of indomethacin at acidic conditions may translate its efficiency to disrupt the gastric surface layer with a consequent decrease in the protection against luminal acid.

In conclusion, this work can contribute to correlate biophysical parameters from the NSAIDs-membrane interactions with their toxicity and therapeutic effects, hence allowing the future development of more selective drugs, diminishing the undesirable side-effects.

## ACKNOWLEDGMENTS AND DISCLOSURES

Cláudia Nunes and Marina Pinheiro thank FCT (Fundação para a Ciência e Tecnologia) for the Post-Doc Grant (SFRH/BPD/81963/2011) and Doc Grant (SFRH/BD/63318/2009), respectively.

## REFERENCES

1. Lucio M, Lima JLFC, Reis S. Drug-membrane interactions: significance for medicinal chemistry. *Curr Med Chem*. 2010;17(17):1795–809.
2. Escriba PV. Membrane-lipid therapy: a new approach in molecular medicine. *Trends Mol Med*. 2006;12(1):34–43.
3. Seydel JK, Wiese M. Drug-membrane interactions: Analysis, drug distribution, modeling, Wiley-VCH, 2002.
4. Weissig V. Liposomes methods and protocols. London: Humana Press; 2010.
5. Lichtenberger LM, Zhou Y, Dial EJ, Raphael RM. NSAID injury to the gastrointestinal tract: evidence that NSAIDs interact with phospholipids to weaken the hydrophobic surface barrier and induce the formation of unstable pores in membranes. *J Pharm Pharmacol*. 2006;58(11):1421–8.
6. Lucio M, Ferreira H, Lima JLFC, Matos C, de Castro B, Reis S. Influence of some anti-inflammatory drugs in membrane fluidity studied by fluorescence anisotropy measurements. *Phys Chem Chem Phys*. 2004;6(7):1493–8.
7. Lucio M, Nunes C, Gaspar D, Golebska K, Wisniewski M, Lima JLFC, et al. Effect of anti-inflammatory drugs in phosphatidylcholine membranes: a fluorescence and calorimetric study. *Chem Phys Lett*. 2009;471(4–6):300–9.
8. van den Hoven JM, Van Tomme SR, Metselaer JM, Nuijen B, Beijnen JH, Storm G. Liposomal drug formulations in the treatment of rheumatoid arthritis. *Mol Pharm*. 2011;8(4):1002–15.
9. Lichtenberger LM. Where is the evidence that cyclooxygenase inhibition is the primary cause of nonsteroidal anti-inflammatory drug (NSAID)-induced gastrointestinal injury? Topical injury revisited. *Biochem Pharmacol*. 2001;61(6):631–7.
10. van Meer G, Voelker DR, Feigenson GW. Membrane lipids: where they are and how they behave. *Nat Rev Mol Cell Biol*. 2008;9(2):112–24.
11. Escriba PV, Gonzalez-Ros JM, Goni FM, Kinnunen PKJ, Vigh L, Sanchez-Magraner L, et al. Membranes: a meeting point for lipids, proteins and therapies. *J Cell Mol Med*. 2008;12(3):829–75.
12. Kaneko T, Matsui H, Shimokawa O, Nakahara A, Hyodo I. Cellular membrane fluidity measurement by fluorescence polarization in indomethacin-induced gastric cellular injury *in vitro*. *J Gastroenterol*. 2007;42(12):939–46.
13. Lichtenberger LM, Zhou Y, Jayaraman V, Doyen JR, O'Neil RG, Dial EJ, et al. Insight into NSAID-induced membrane alterations, pathogenesis and therapeutics: Characterization of interaction of NSAIDs with phosphatidylcholine. *Biochim Biophys Acta-Mol Cell Biol Lipids*. 2012;1821(7):994–1002.
14. Lichtenberger LM, Wang ZM, Romero JJ, Ulloa C, Perez JC, Giraud MN, et al. Non-steroidal anti-inflammatory drugs (NSAIDs) associate with zwitterionic phospholipids: insight into the mechanism and reversal of NSAID-induced gastrointestinal injury. *Nat Med*. 1995;1(2):154–8.
15. Lichtenberger LM, Graziani LA, Dial EJ, Butler BD, Hills BA. Role of surface-active phospholipids in gastric cytoprotection. *Science*. 1983;219(4590):1327–9.
16. Lichtenberger LM. The hydrophobic barrier properties of gastrointestinal mucus. *Annu Rev Physiol*. 1995;57:565–83.
17. Brzozowski T. Nonsteroidal anti-inflammatory drug-induced experimental gastropathy: is gastric acid the major trigger? *Clin Exp Pharmacol Physiol*. 2010;37(7):651–3.
18. da Silva AMG, Romao RIS. Mixed monolayers involving DPPC, DODAB and oleic acid and their interaction with nicotinic acid at the air-water interface. *Chem Phys Lipids*. 2005;137(1–2):62–76.
19. Allen A, Pearson JP. The gastrointestinal adherent mucous gel barrier. In: Corfield AP, editor. Glycoprotein methods and

- protocols - The Mucins, Vol. 125. Totowa: Humana Press; 2000. p. 57–64.
20. Mosnier P, Rayssiguier Y, Motta C, Pelissier E, Bommelaer G. Effect of ethanol on rat gastric surfactant: a fluorescence polarization study. *Gastroenterology*. 1993;104(1):179–84.
  21. Jordan O, Butoescu N, Doelker E. Intra-articular drug delivery systems for the treatment of rheumatic diseases: a review of the factors influencing their performance. *Eur J Pharm Biopharm*. 2009;73(2):205–18.
  22. Ferreira H, Lúcio M, Lima JLFC, Cordeiro-da-Silva A, Tavares J, Reis S. Effect of anti-inflammatory drugs on splenocyte membrane fluidity. *Anal Biochem*. 2005;339(1):144–9.
  23. Gaspar D, Lucio M, Wagner K, Brezesinski G, Rocha S, Lima JLFC, *et al*. A biophysical approach to phospholipase A(2) activity and inhibition by anti-inflammatory drugs. *Biophys Chem*. 2010;152(1–3):109–17.
  24. Sousa C, Nunes C, Lucio M, Ferreira H, Lima JLFC, Tavares J, *et al*. Effect of nonsteroidal anti-inflammatory drugs on the cellular membrane fluidity. *J Pharm Sci*. 2008;97(8):3195–206.
  25. Nunes C, Brezesinski G, Pereira-Leite C, Lima JLFC, Reis S, Lucio M. NSAIDs interactions with membranes: a biophysical approach. *Langmuir*. 2011;27(17):10847–58.
  26. Pereira-Leite C, Nunes C, Lima JLFC, Reis S, Lucio M. Interaction of celecoxib with membranes: the role of membrane biophysics on its therapeutic and toxic effects. *J Phys Chem B*. 2012;116(46):13608–17.
  27. Nunes C, Brezesinski G, Lima JLFC, Reis S, Lucio M. Synchrotron SAXS and WAXS study of the interactions of NSAIDs with lipid membranes. *J Phys Chem B*. 2011;115(24):8024–32.
  28. Nunes C, Brezesinski G, Lopes D, Lima JLFC, Reis S, Lucio M. Lipid-drug interaction: biophysical effects of tolmetin on membrane mimetic systems of different dimensionality. *J Phys Chem B*. 2011;115(43):12615–23.
  29. Panicker L, Mishra KP. Influence of salicylic acid on the biophysical properties of dipalmitoyl phosphatidylcholine vesicles. *Phase Transit*. 2008;81(1):65–76.
  30. Balimane PV, Chong SH, Morrison RA. Current methodologies used for evaluation of intestinal permeability and absorption. *J Pharm Toxicol Methods*. 2000;44(1):301–12.
  31. Ho C, Slater SJ, Stubbs CD. Hydration and order in lipid bilayers. *Biochemistry-U.S.* 1995;34(18):6188–95.
  32. Lasic DD, Needham D. The “stealth” liposome: a prototypical biomaterial. *Chem Rev*. 1995;95:2601–28.
  33. Hope MJ, Bally MB, Webb G, Cullis PR. Production of large unilamellar vesicles by a rapid extrusion procedure. Characterization of size distribution, trapped volume and ability to maintain a membrane potential. *Biochim Biophys Acta*. 1985;812:55–65.
  34. Savitzky A, Golay MJE. Smoothing and differentiation of data. *Anal Chem*. 1964;36:1627–39.
  35. Magalhaes LM, Nunes C, Lucio M, Segundo MA, Reis S, Lima JLFC. High-throughput microplate assay for the determination of drug partition coefficients. *Nat Protoc*. 2010;5(11):1823–30.
  36. Coutinho A, Prieto M. Ribonuclease T1 and alcohol dehydrogenase fluorescence quenching by acrylamide. *J Chem Educ*. 1993;70:425.
  37. Amin K, Wasan KM, Albrecht RM, Heath TD. Cell association of liposomes with high fluid anionic phospholipid content is mediated specifically by LDL and its receptor, LDLr. *J Pharm Sci*. 2002;91(5):1233–44.
  38. Koynova R, Koumanov A, Tenchov B. Metastable rippled gel phase in saturated phosphatidylcholines: calorimetric and densitometric characterization. *Bba-Biomembr*. 1996;1285(1):101–8.
  39. Chakraborty H, Roy S, Sarkar M. Interaction of oxamic NSAIDs with DMPC vesicles: differential partitioning of drugs. *Chem Phys Lipids*. 2005;138(1–2):20–8.
  40. Kundu S, Chakraborty H, Sarkar M, Datta A. Interaction of Oxamic NSAIDs with lipid monolayer: anomalous dependence on drug concentration. *Colloid Surface B*. 2009;70(1):157–61.
  41. Lozano HR, Martínez F. Thermodynamics of partitioning and solvation of ketoprofen in some organic solvent/buffer and liposome systems. *Braz J Pharm Sci*. 2006;42(4):601–13.
  42. Lakowicz JR. Principles of fluorescence spectroscopy. New York: Springer; 2006.
  43. Illinger D, Duportail G, Mely Y, Poirelmoales N, Gerard D, Kuhry JG. A comparison of the fluorescence properties of Tma-Dph as a probe for plasma-membrane and for endocytic membrane. *Bba-Biomembr*. 1995;1239(1):58–66.
  44. Kovacs E, Savopol T, Iordache MM, Saplacan L, Sobaru I, Istrate C, *et al*. Interaction of gentamicin polycation with model and cell membranes. *Bioelectrochemistry*. 2012;87:230–5.
  45. Monteiro JP, Martins AF, Lucio M, Reis S, Pinheiro TJJ, Galdes CFGC, *et al*. Nimesulide interaction with membrane model systems: are membrane physical effects involved in nimesulide mitochondrial toxicity? *Toxicol Vitro*. 2011;25(6):1215–23.
  46. Monteiro JP, Martins AF, Lucio M, Reis S, Galdes CFGC, Oliveira PJ, *et al*. Interaction of carbonylcyanide p-trifluoromethoxyphenylhydrazone (FCCP) with lipid membrane systems: a biophysical approach with relevance to mitochondrial uncoupling. *J Bioenerg Biomembr*. 2011;43(3):287–98.
  47. Brittes J, Lucio M, Nunes C, Lima JLFC, Reis S. Effects of resveratrol on membrane biophysical properties: relevance for its pharmacological effects. *Chem Phys Lipids*. 2010;163(8):747–54.